AN ASYMPTOTIC ANALYSIS OF METHODS FOR PREDICTING THE FRACTURE TOUGHNESS OF MULTIAXIAL CARBON FIBER COMPOSITE LAMINATES USING THE ELASTIC CONSTANTS OF THE 0º PLIES

M. Y. Abdellah   UDC 539.4

Carbon fiber composite laminates are an important alternative to metal in many mechanical structural applications. Carbon fiber composite laminates usually have multidirectional plies with different angles. In this study, a simple analytical model is derived to predict the notch strength of these multidirectional plies from the unidirectional strength of the 0º ply. The first method considers the orthogonal analysis of the forces introduced in each ply at the Cartesian coordinates in each of the 2 axes with their direction, and then calculates the resulting forces. The second method considers the percentage of layers inside the laminates and then orthogonally analyzes the induced forces on the entire laminate sheets. The resulting stress induced by these forces is calculated according to the theory of maximum failure shear or principal stress. In addition, the fracture toughness G_{IC} was predicted based on the strength of the unnotched laminates calculated by previous methods. In addition, the size effect of the open-hole specimen was measured based on the predicted fracture toughness and strength of the unnotched laminates. The model was compared with available experimental and other published models. The optimum values for the two methods of fracture toughness were determined. The average percent accuracy of size effect prediction based on the first method is 3.24%, while it is 6.82% for the second method.

***Keywords*:** ply, layup, nominal strength, unidirectional, multidirectional.

Nomenclature

σ_{un}, σ_{la}	–	un-notch strength
$\overline{A_{90}}, \overline{A_{\theta}}$, and $\overline{A_0}$	–	area of laminate in 90º, angle ply, and 0º
$\overline{A_{lay}}, \overline{A_{ply}}$, and $\overline{A_{lax}}$	–	area of laminate in y, angle ply, and in x
$[A]$	–	stiffness matrix
A_{90}	–	area of 90º ply
A_{la}	–	area of laminate
A_{ply} and A_{plx}	–	area of ply in x and y directions
A_{θ}	–	area of angle ply
E_1, E_2, G_{12}, and ν_{12}	–	elastic constant in 1 and 2 principal directions
E_{eff}	–	modified effective Young modulus
E_x, E_y, G_{xy}, and ν_{xy}	–	elastic constant in x and y Cartesian coordinates
F_0	–	force induced in zero direction

Mechanical Engineering Department, Faculty of Engineering, South Valley University, Qena, Egypt. Mechanical Engineering Department, College of Engineering and Islamic Architecture, Umm Al-Qura University, Makkah, KSA (myahmad@uqu.edu.sa; mohamed_abdalla@eng.svu.edu.eg).

F_{lay}	–	ply force induced in y direction
F_x and F_y	–	total component of force in x and y directions
F_θ	–	force induced in angle direction
I_1	–	ones matrix
Q_{xy}	–	the reduced stiffness
X_t and X_c	–	uniaxial tensile and compression strength
f_{ij}	–	transformation function calculating in Appendix [1]
δ_c	–	critical crack opening
δ_{ij}	–	Kronecker delta
ε_f	–	fracture strain
λ_{90}, λ_θ, and λ_0	–	percent of ply in 90º, angle, and 0º, respectively
$\bar{\sigma}$	–	average stress
σ_{90}	–	uniaxial stress in 90º ply
σ_{lay}	–	stress through laminates in y direction
σ_n	–	nominal strength
σ_θ	–	uniaxial stress through angle ply
G_{IC}	–	mode I fracture toughness, kJ/m^2
x and y	–	Cartesian coordinates
ψ	–	calculated equivalent Young modulus
N	–	total number of plies
nx	–	number of ply in x direction
ny	–	number of plies in y direction
t	–	total thickness of laminate
θ	–	angle of ply inclination

Introduction. Carbon fiber composite laminate structures are a competitive alternative to many metals due to their excellent specific strength and specific weight, especially in the aerospace, marine and offshore industries [2–4]. In the design of such materials, stress concentration factors [5] are usually used, which are caused by discontinuity or interfaces between plies or layers such as delaminations [6]. Therefore, the applicability of such types of materials depends mainly on a fast and robust model to determine their strength under accurate applications.

Finite element methods can predict the strength of laminates with good accuracy, but they are time consuming and not preferable in optimization [5, 7] or material selection proposals [8]. Moreover, most mesh element methods need to be refined, which increases the computation time. Therefore, analytical methods based on the cohesive zone model can be proposed and overcome the limitation of FEM difficulties with satisfactory accuracy and speed [9–11]. A direct relationship between the fracture toughness and the notched impact strength of a structural plate was established by Tan [12]. The cohesive zone model uses a fictitious crack [13] and relates the cohesive stress across the crack surface and the critical crack opening [14]. The cohesive zone model used to predict the nominal strength of composite laminates with open holes can have different forms: linear [9], exponential [1] and even bilinear [15]. Fracture toughness for aerospace and aircraft wings should be precisely defined to improve safety [16]. Therefore, to define it completely, two main parameters are required: fracture toughness and notched impact strength of composite laminates. Many analytical models [1, 17–19] have been derived to predict the nominal strength of cracked composite laminates. The failure modes would be concentrated in a process zone ahead of the crack tip if the thickness of the plies is sufficiently thin, while for thicker plies, failure occurs by delamination. For composite structures, the nominal strength decreases as the size or geometry of the structure increases [20]. Therefore, in order to predict the size effect well, methods are needed to calculate the energy lost due to crack propagation [21].

Furtado et al. [5] proposed an analytical model to predict the strength of open hole carbon fiber reinforced polymer laminates. This model used three characteristic material properties such as fracture toughness, Young's modulus and notched impact strength, these parameters were calculated using invariant-based models, the results were acceptable, but the model lacks generality of layers and stacking sequences with large percentage error, neglecting the availability of many angular layers with 90° or without. In this context, it was reported in [22] that the longitudinal fracture toughness of Hexcel IM7-8552 carbon epoxy multidirectional laminates can be predicted using unidirectional laminates based on linear elastic fracture mechanics (LEFM) concepts and lamination theories, but the accuracy of these models required increasing caution and more experience to be implemented. Therefore, a simplification based on geometry and orientation was performed by Mohammed et al [23]. In addition, a comparative study was presented by Abdellah [24] to predict the fracture toughness of T800/924C CFRP. Here, the cohesive zone model was applied in reverse to predict the fracture toughness with the definition of the size-effect curve profile of the open-hole specimen, and the results were compared with the results of the study by Soutis and Curtis [25], in which the nominal strength of open-hole specimens was predicted using the cohesive zone model based on the experimentally measured fracture toughness and a predicted notch-free strength. Since the two parameters of the cohesive zone model are a characteristic property, it was not necessary to measure each time the specimen geometry changed due to holes, cracks, or other shape discontinuities. Moreover, the cohesive zone models are based on physical properties with exact sense [26].

The linear elastic failure theories for isotropic material have been used [27–30] to predict the failure of composite materials, but their applicability and reliability are still problematic and require much work. Micromechanical models have been used to accurately predict the stiffness and strength models of composite laminates using length, stochastic fiber orientation, fiber volume fraction, and void volume fraction [31]. The strain energy failure criterion has been used to predict the tensile strength of composite laminates, but was limited to some assumptions. Recently, natural vibration was used as a nondestructive test [32] o measure the fracture toughness and size effect of composite laminates. In the study, the equivalent Young modulus of the glass fiber composite structure was first predicted from the natural frequencies, and then the modified hook law was used according to the LEFM approach with high accuracy and lower % error.

It is clear that the elasticity theories need to be further investigated in order to apply them in the calculation of strength and elastic stiffness of composite laminates. Therefore, the present study attempts to establish a robust model to predict the notch-free strength of laminates with angular plies and quasi-isotropic plies, and to propose a model to predict the fracture toughness of composite laminates and the strength of CFRP composite panels with open holes. Another objective of the present study is to compare the results of the proposed models with other available models to determine the optimization and accuracy of the model. In addition, the size-response curve of the open-hole sample is determined.

In the first section, the analytical model is explained, and in the second section, the results of the model are compared with those of other publications to obtain optimization tables. Finally, the results are summarized.

1. Un-Notch Strength. The following macromechanical analysis method is an attempt to calculate the strength σ_{un} of unidirectional composite laminates from the strength of unidirectional laminates in tension X_t or in compression X_c. Then the equivalent Young modulus is calculated using the stiffness of unidirectional laminates E_1, E_2, ν_{12}, and G_{12}. Based on the prediction of multidirectional strength without notch, fracture strain and equivalent Young modulus, it is possible to calculate fracture toughness G_{IC} by theories of elastic fracture mechanics. Finally, the size effect of open holes can be predicted using the linear cohesive law.

1.1. Method 1-a. Simple method based on equilibrium forces in each ply for balanced laminates with θ-angle, 0° and 90° ply. The problem is divided into four segments (top and bottom) in the y-axis direction and (right and left) in the x-axis direction, as shown in Fig. 1. The positive direction is clockwise.

Analysis the forces in only y directions without consider forces in x direction (Fig. 1a) as follows:

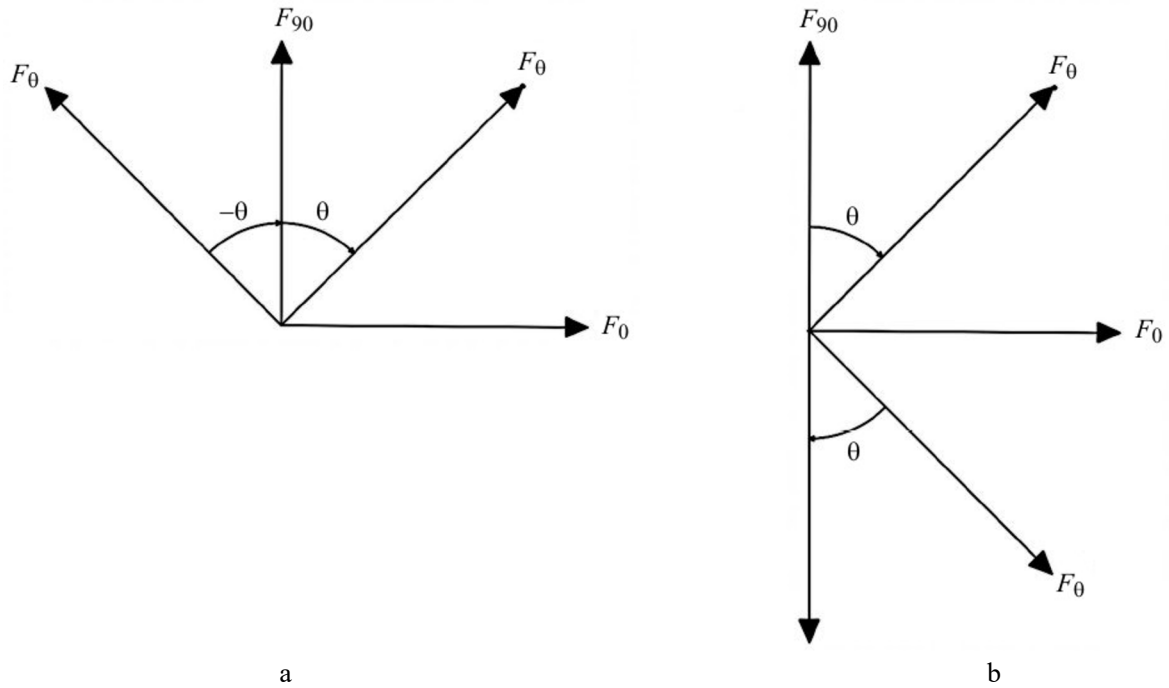$$F_{lay} = \sum F_y = F_0 + F_\theta \cos(\theta) + F_\theta \cos(\theta), \tag{1}$$

Fig. 1. Cartesian coordinates of multidirectional laminates with θ-angle position: (a) upper and lower segment; (b) right and left segment.

where F_{lay} is the total laminates force in y direction. As the force through fiber is equal the stress through laminates multiplied by area $\sigma_{lay} A_{la}$ therefore the previous equation can be rewritten as

$$\sigma_{lay} A_{la} = \sum F_y A_{ply} = \sigma_{90} A_{90} + \sigma_\theta A_\theta \cos(\theta) + \sigma_\theta A_\theta \cos(\theta), \qquad (2)$$

where A_{la} is laminate area per unit width equal ($A_{la} = Nt$), where t is laminates thickness, N is total laminates plies, and A_{ply} ply area which equal to ($A_{ply} = (N/ny)t$). Therefore, substitution into Eq. (2) give the following expression:

$$\sigma_{lay} = \sum F_y A_{ply} = \frac{\sigma_{90}}{ny} + \frac{\sigma_\theta}{ny} \cos(\theta) + \frac{\sigma_\theta}{ny} \cos(\theta), \qquad (3)$$

where ny is total ply in y direction which is equal to ($ny = \sum(n_{90} + n_\theta)$), where n_{90} and n_θ are 90° and θ plies, respectively. Repeat the pervious analysis at the bottom side of the laminates.

The same analysis is carried out for the right and lift section in x direction of the laminates (Fig. 1b), it is obtained the strength in x direction as follows:

$$\sigma_{lax} = \sum F_x A_{plx} = \frac{\sigma_0}{nx} + \frac{\sigma_\theta}{nx} \sin(\theta) + \frac{\sigma_\theta}{nx} \sin(\theta), \qquad (4)$$

where nx is total ply in x direction which is equal to ($nx = \sum(n_0 + n_\theta)$), where n_0 and n_θ are 0° and θ plies, respectively. Then the multidirectional laminate strength (σ_{la}) is the product of the strengths in the y and x direction as follows:

$$\sigma_{la} = 2\sqrt{\sigma_{lax}^2 + \sigma_{lay}^2}. \qquad (5)$$
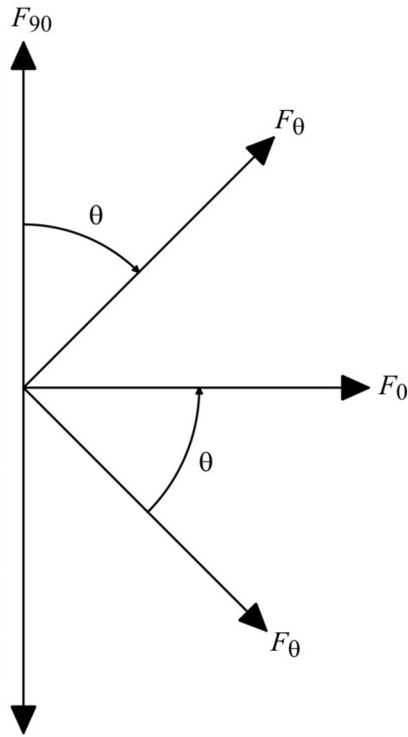
1033

Fig. 2. Cartesian coordinates of multidirectional laminates with θ angle ply.

1.2. Method 1-b. For laminates without 90º or without θ, the Cartesian coordinate from Fig. 2 is used. And the thickness of the laminates can be calculated as follows:

For strength in y direction, it is as follows:

$$\sigma_{lay} = \sum F_y A_{ply} = \sigma_{90}\lambda_{90} + \sigma_\theta \lambda_\theta \cos(\theta) + \sigma_{-\theta}\lambda_{-\theta}\cos(2\pi - \theta). \tag{6}$$

For strength in x direction, it is as follows:

$$\sigma_{lax} = \sum F_x A_{plx} = \sigma_0 \lambda_0 + \sigma_\theta \lambda_\theta \sin(\theta) + \sigma_{-\theta}\lambda_{-\theta}\sin(2\pi - \theta). \tag{7}$$

The laminates consider one plate with x, y component and the resultant force is as follows:

$$\sigma_{la} = 2\sqrt{\sigma_{lax}^2 + \sigma_{lay}^2}. \tag{8}$$

Here $\lambda_{90}, \lambda_0, \lambda_\theta$, and $\lambda_{-\theta}$ are percent of 90º, 0º, and $\pm\theta$ ply in the whole laminates thickness.

1.3. Method 2. This method is similar to method 1-b, but is considered a general method for quasi-isotropic laminates with all stacking sequences, based on orthogonal force analysis of two sides of the laminates and ply percentages through the laminates. Both maximum principal stress theory and maximum shear stress theory are used. Referring to Fig. 2, the force analysis is as follows:

$$F_{lay} = \sum F_y = F_{90} + F_\theta \cos(\theta) + F_\theta \cos(2\pi - \theta). \tag{9}$$

1034

And the x component of force is as follows:

$$F_{lax} = \sum F_x = F_0 + F_\theta \sin(\theta) + F_\theta \sin(2\pi - \theta). \tag{10}$$

By substituent stress σ instead of forces, these equations can be rewritten as follows:

$$\sigma_{lay} \times \overline{A_{lay}} = \sum F_y \overline{A_{ply}} = \sigma_{90}\overline{A_{90}} + \sigma_\theta \overline{A_\theta}\cos(\theta) + \sigma_\theta \overline{A_\theta}\cos(2\pi - \theta), \tag{11}$$

where $\overline{A_{la}}$ is the total laminate area per unit width and equal to $\overline{A_{lay}} = (\lambda_{90} + \lambda_\theta + \lambda_{-\theta} + \lambda_0)t$ also $\overline{A_{lax}} = (\lambda_{90} + \lambda_\theta + \lambda_{-\theta} + \lambda_0)t$ and $\overline{A_{ply}}$ ply area per width which equal to $(\overline{A_{ply}} = (N_{ply}/N)t = \lambda_{ply}t)$. Therefore, substitution into Eq. (11) give the following expression:

$$\sigma_{lay} = \sum F_y \overline{A_{ply}} = \sigma_{90}\lambda_{90} + 2\sigma_\theta \lambda_\theta \cos(\theta) + 2\sigma_\theta\lambda_{-\theta} \cos(2\pi - \theta). \tag{12}$$

Repeat the steps for the x direction, it is obtained the following expression:

$$\sigma_{lax} = \sum F_y \overline{A_{plx}} = \sigma_0\lambda_0 + 2\sigma_\theta \lambda_\theta \cos(\theta) + 2\sigma_\theta\lambda_{-\theta} \cos(2\pi - \theta). \tag{13}$$

Note the number 2 is used to obtain to sides of the laminates right and left segments.

Then the maximum failure shear stress theory can be applied [25, 30, 33] for some quasi-isotropic laminates to obtain the resultant strength as follows:

$$\sigma_{la} = \frac{\sigma_{lay} - \sigma_{lax}}{2}, \tag{14}$$

or the maximum principal failure stress theory can be expressed as follows:

$$\sigma_{la} = \frac{\sigma_{lay} + \sigma_{lax}}{2}. \tag{15}$$

2. Fracture Toughness. The fracture toughness G_{IC} is an important property to obtain the size-response curve or to predict the nominal strength of composite plates with open holes using the cohesion law [1, 22, 23]. The cohesive law relates the strength σ at the onset of failure to the progressive crack opening δ [10, 34, 35], as shown in Fig. 3. The notch-free failure strength of laminates for which σ_{la} was previously measured is related to the GIC by linear cohesion laws as follows [24, 25]:

$$G_{Ic} = \int_0^{\delta_c} \sigma_{la}d\delta = \sigma_{la}\delta_c. \tag{16}$$

Now the critical crack opening displacement δ_c can be calculated using the proposed equation by Hahn and Rosenfield [36] and Perez [37], under the following stress condition at fracture:
For plan stress condition:

$$\delta_c = t\varepsilon_f. \tag{17}$$

For plane strain condition:
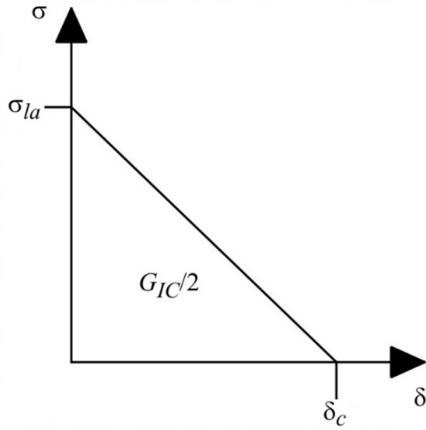
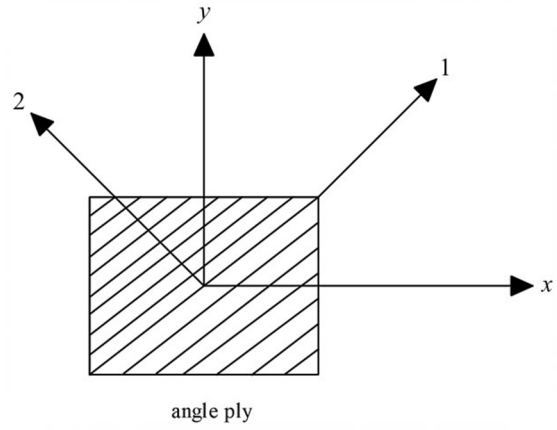$$\delta_c = t\varepsilon_f(1 - v_{xy}^2). \tag{18}$$

Fig. 3. Linear cohesive law.

Fig. 4. Angle ply transformation system.

To calculate the strain at break ε_f, the equivalent Young modulus ψ is first calculated from the unidirectional elastic stiffness of unidirectional laminates using lamination theories. The indices 1 and 2 represent the lamina properties in the fiber direction and in the transverse direction, respectively [38] (see Fig. 4). The reduced stiffness [39] Q_{ij} can be expressed by the elastic constant of the laminae as follows:

$$Q_{11} = \frac{E_1}{1 - v_{12}v_{21}}, \qquad Q_{22} = \frac{E_{12}}{1 - v_{12}v_{21}},$$

$$Q_{12} = \frac{v_{12}E_2}{1 - v_{12}v_{21}}, \quad Q_{66} = G_{12}, \quad v_{21} = v_{12}\frac{E_2}{E_1}. \tag{19}$$

For symmetric layup, the average stress $\bar{\sigma}$ through laminates thickness t can be calculated using Eqs. (20):

$$\bar{\sigma} = [A]\frac{\{\epsilon\}}{t}, \quad \begin{pmatrix} \bar{\sigma}_x \\ \bar{\sigma}_y \\ \bar{\sigma}_z \end{pmatrix} = \begin{pmatrix} A_{11} & A_{12} & A_{16} \\ A_{12} & A_{22} & A_{26} \\ A_{16} & A_{26} & A_{66} \end{pmatrix} \begin{pmatrix} \varepsilon_x \\ \varepsilon_y \\ \varepsilon_z \end{pmatrix}, \tag{20}$$

where A is the stiffness matrix where can calculate from the following relationship [Eqs. (21)] for multidirectional laminates with θ angle plies:

$$A_{11} = A_{11}^{90} + A_{11}^{0} + A_{11}^{\theta}, \quad A_{22} = A_{22}^{90} + A_{22}^{0} + A_{22}^{\theta},$$

$$A_{12} = A_{12}^{90} + A_{12}^{0} + A_{12}^{\theta}, \quad A_{66} = A_{66}^{90} + A_{66}^{0} + A_{66}^{\theta},$$

$$A_{ij}^{90} = \lambda_{90}Q_{ij}t_{90}, \quad A_{ij}^{0} = \lambda_{0}Q_{ij}t_{0}, \quad A_{11}^{\theta} = \lambda_{\theta}\left(\frac{Q_{11}}{4} + \frac{Q_{22}}{4} + \frac{Q_{12}}{4} + Q_{66}\right)t_{\theta} = A_{22}^{\theta}, \tag{21}$$

$$A_{12}^{\theta} = \lambda_{\theta}\left(\frac{Q_{11}}{4} + \frac{Q_{22}}{4} + \frac{Q_{12}}{4} - Q_{66}\right)t_{\theta}, \quad A_{66}^{\theta} = \lambda_{\theta}\left(\frac{Q_{11}}{4} + \frac{Q_{22}}{4} - \frac{Q_{12}}{2}\right)t_{\theta},$$

where t_{90}, t_0, and t_θ are ply thickness of 90°, 0°, and θ direction, respectively.

Substitution into Eqs. (22) give an expression for elastic constant in x and y directions:

$$E_x = A_{11} - \frac{A_{12}^2}{A_{22}}, \qquad E_y = A_{22} - \frac{A_{12}^2}{A_{11}}, \qquad G_{xy} = A_{66}, \qquad v_{xy} = \frac{A_{12}}{A_{22}}. \tag{22}$$

1036

Then after the elastic constant in x, y directions calculated the equivalent Young modulus is then can be determine form Eqs. (23) as follows:

$$\psi = \frac{\sqrt{2E_x E_y}}{\sqrt{\sqrt{\frac{E_y}{E_x} + \frac{E_y}{2G_{xy}} - \nu_{xy}}}}.$$ (23)

Substitution into Hooke's law for linear material behaviors into Eq. (24) as follows:

$$\varepsilon_f = \frac{\sigma_{la}}{\psi}.$$ (24)

To evaluated the effective Young modulus E_{eff}, rearrange Eq. (16) and modification respect to (17), it is given Eq. (25) as follows:

$$E_{eff} = \frac{\sigma_{la}^2}{G_{IC}} t.$$ (25)

3. Nominal Strength and Size Effect. The linear cohesion law, shown in Fig. 3, is used to determine the nominal strength of open hole specimens of carbon fiber laminates. The two main parameters fracture toughness GIC and laminate strength σ_{la} determined in the previous sections must be fully described and defined, then Eq. (26) [9, 10] is applied as follows:

$$\sigma_n = \delta_c \left[\frac{\delta_c}{\sigma_{la}} \delta_{ij} + f_{ij} \right]^{-1} I_1,$$ (26)

where δ_{ij} is knocker delta and I_1 is one matrix, and f_{ij} is the transformation function completely derived in [9, 10].

4. Results and Discussion. Figures 5 and 6 and Table 1 show the predicted failure strength of multidirectional laminates. It can be observed that the percent error in tension is 4.37 and –2.72 for La0 and 9.297 and 1.897 for La1 for method a1 and method 2, respectively; moreover, the percent error is 0.70 and –6.13 for La2. For compression, these values increase to –14.63 and –20.45, respectively. The same results for compression for the other material La1, as the percent errors are 17.439 and 9.461 for method a1 and method 2, respectively. The average percent errors for all materials (La0, La1, and La2) in tension and compression were 9.29 and 8.13 for method 1-a and method 2, respectively, which is based on the maximum shear stress theory. These values are lower than the average percent error of 9.8 produced by other unit circle models [5].

TABLE 1. Comparison of Predicted Failure Strength of Quasi-Isotropic Laminates Using the Present Models with Experimental and Other Available Published Models for Different CFRP Material Systems with Layered Structure {Maximum Shear Stress [Eq. (15)]}

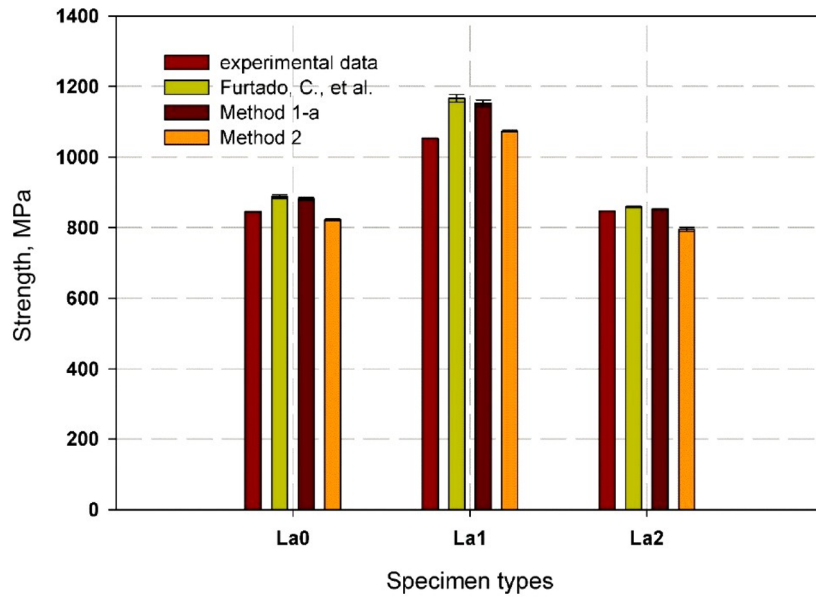| #	Material	Layup	0º ply strength (MPa)	Multiaxial laminates strength (MPa)			
				Exp.	Model other [5]	Method 1-a, Eq. (5)	Method 2
La0	IM7/8552 [5, 33]	[90/0/±45]₃ₛ	2326	845	888	882	822
			1200 (–)	533	458	455	424
La1	T800/M21 [5, 19]	[90/45/0/–45]₃ₛ	3039	1054	1166	1152	1074
			1669 (–)	539	637	633	590
La2	M40JB/ThinPreg 80EP/CF [40, 44]	[(0/90)/(45/–45)]₃ₛ	2250	847	859	853	795
			1052 (–)	–	402	399	371

Fig. 5. Comparison model methods with experimental data [5, 19, 33, 40, 44] and other available models [5] in tension case for CFRP.
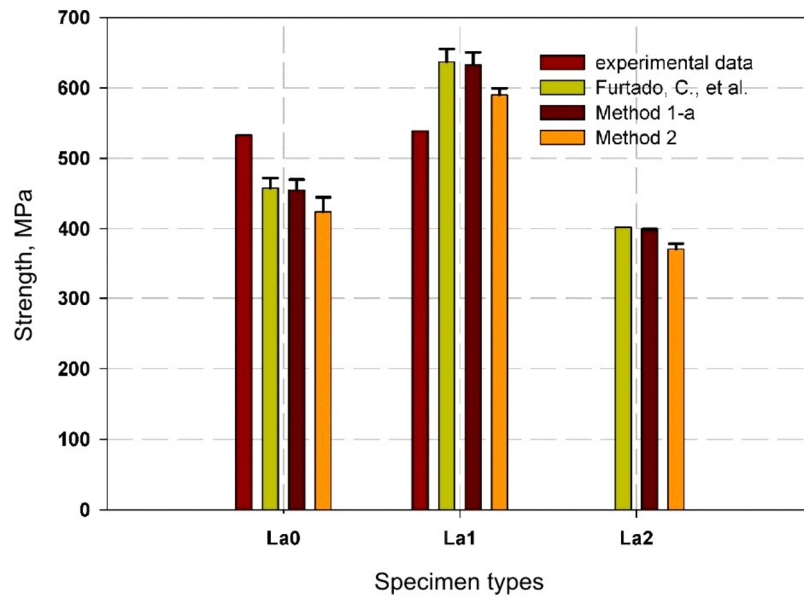

Fig. 6. Comparison among model methods with experimental data [5, 19, 33, 40, 44] and other available models [5] in compression based on Eq. (15).

Figure 7 and Table 2 show the failure strength predicted by method 1-a and method 2, which is based on maximum principal stress theory, for CFRP laminates under compression. The percent errors for La3 are –0.97 and 5.24 for method 1-a and method 2, respectively, which is based on maximum principal stress theory. This theory was selected for these material systems with relatively lower fracture toughness than those listed in Table 1. It is found that La5 has a lower % error –0.82 when method 1-a is used, while the % error increases by 57% for method 2. However, moderate % errors –17.53 and 10.61 were observed for sample La4. This result is due to unbalanced stacking sequences. In general, method 1-a gives the lowest average % error –6.44 corresponding to 11.092 for the model of Soutis and Curtis [25].

1038

TABLE 2. Comparison of Predicted Failure Strength of Quasi-Isotropic Laminates Using the Present Models with Experimental and Other Available Published Models for Different CFRP Material Systems with Layered Structure {Maximum Principal Stress [Eq. (16)]}

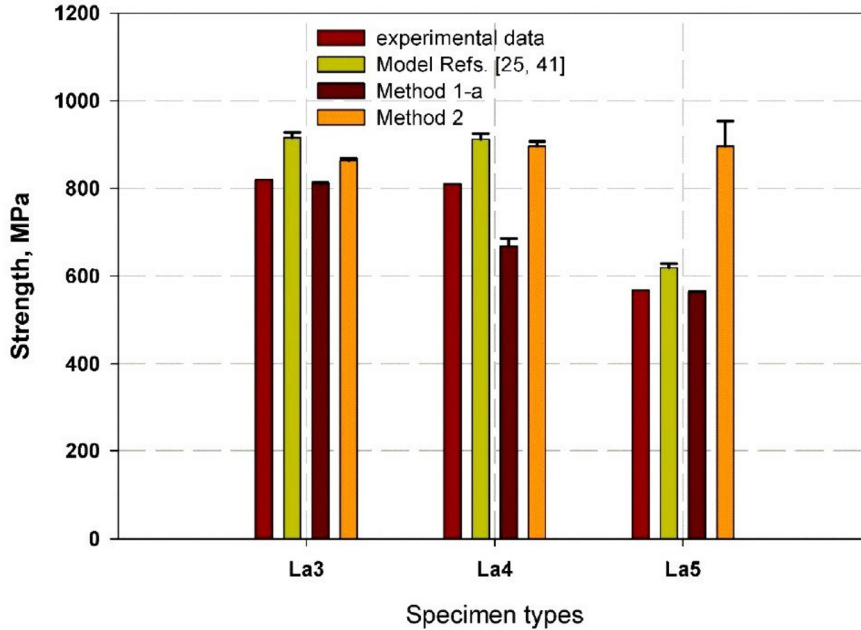| #	Material	Layup	0º ply strength (MPa)	Multiaxial laminates strength (MPa)			
				Exp.	Model other [5]	Method 1-a, Eq. (5)	Method 2
La3	T800/924C	$[\pm 45/0_2/90_2/0_2/90_2/0_2]_s$	1485 (−1)	820	916	812	863
La4	[25, 41]	$[(\pm 45/0_2)]_{3s}$	1485 (−1)	810	912	668	896
La5		$[(\pm 45/0/90)_3]_s$	1485	568	619	563.34	896

Fig. 7. Comparison among model methods with experimental data [25, 41], and other available models in compression case for CFRP.

Figure 8 and Table 3 show the prediction of the failure strength of CFRP laminates with an angular layer [θ/0]2s or a laminate with only one transverse layer [0/90]. These types of superstructures were calculated using method 1-b because it has the same aspects as method 1-a. The comparison of the percentage error shows that it is generally lower for both methods, but differs for specimen La10 because there is no angular layer to reduce the size effect and balance the loads by a specific direction, since the superstructure has a loss when loaded by the exact direction. The percentage errors were –6.25 and –3.36 for La6, while they were 6.57 and 5.12 for La7, with positive sense, moreover, the percentage errors for La8 and La9 were 4.09, –6.8182 and –2.6, –28.3614 for method 1-b and method 2, respectively. Although the percent error –3.13 in the case of La10 has a lower value for method 2, it is very large at 30% for method 1-b, which can be attributed to the loss of shear load due to arbitrary angular positions [5, 40–43]. Finally, the model within the two methods has a lower average % error of 9.9 and 9.3, while the average % error of the model proposed by Soutis and Curtis[25] is larger at 18.

Table 4 shows the comparison between the predicted fracture toughness measured by the proposed Eq. (16) and the notched impact strength calculated by method 1. It is observed that the percentage errors vary between lower and higher values, with the lowest value of percentage errors being –1.76 and –5.86 for La4 and La5, respectively (see Fig. 9). It is noted that the calculated equivalent ψ for La0 is the same as the values of fracture toughness were used for plane stress condition [Eq. (17)], as it is suitable for high values of fracture toughness for less thin laminates by thickness [24]. The percent errors listed in Table 5 obtained by method 2 generally have lower values for most specimen

types, although the La4 material has the highest value of –19.66 due to its high predicted strength of 896 MPa and therefore does not match its experimental fracture toughness [25] (see Fig. 9). The optimum values for the two methods are listed in Table 6 and Fig. 10. The optimum values are mainly obtained from the second proposed method.

TABLE 3. Comparison of Predicted Failure Strength of T800/ 924C CFRP with $[\theta/0]_{2s}$ and without Angular Laminate Using the Present Models with Experimental and Another Available Published Model

#	Material	Layup	0° ply strength (MPa)	Multiaxial laminates strength (MPa)			
				Exp.	Model other [25, 41]	Method 1-b, Eq. (9)	Max. principal stress, Eq. (16)
La6	T800/924C [25, 41]	$[\pm30/0_2)_2]_s$	1178 (–)	832	995	780	804.0
La7		$[\pm45/0_2)_2]_s$	1298 (–)	745	820	794	783.2
La8		$[\pm60/02)2]_s$	1230 (–)	660	768	687	615.0
La9		$[\pm75/0_2)_2]_s$	1233 (–)	653	757	636	467.8
La10		$[(0/90_2/0)_3]_s$	1298 (–)	670	858	871	649.0

TABLE 4. Comparison of Prediction of Fracture Toughness Based on Un-Notch Strength of Method 1-a

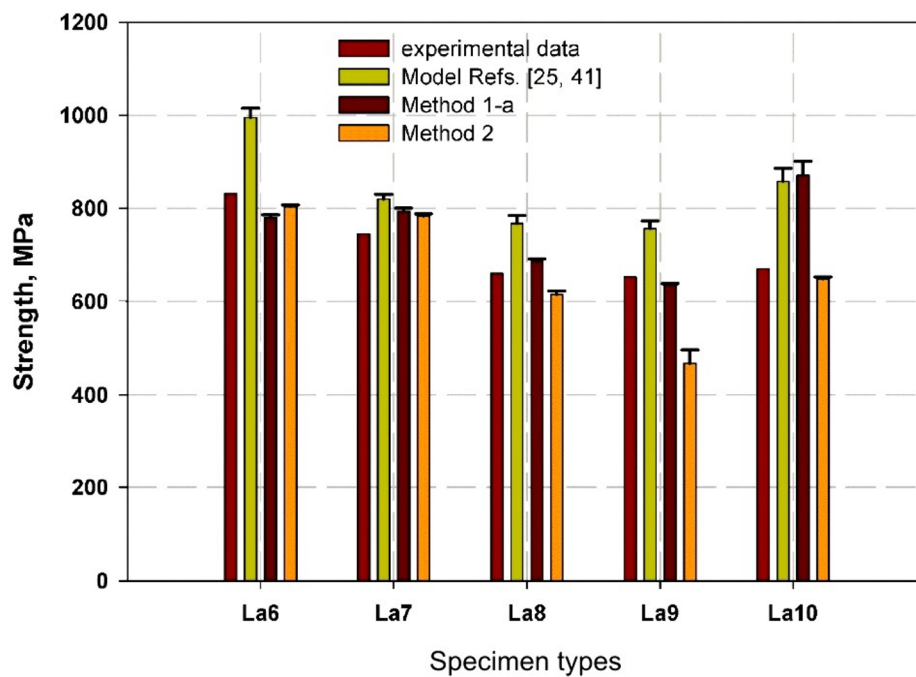| #	Material	Layup	Fracture toughness G_{IC}			ψ (GPa)	E_{eff} (GPa)
			Exp.	Predicted	% error		
La0	IM7/8552 [5, 33]	$[90/0/\pm45]_{3s}$	81.5	100 Eq. (17)	22.69	23.34	23.34
				Eq. (18)			
La3, doubled 0°	T800/924C [25, 41]	$[\pm45/0_2/90_2/0_2/90_2/0_2]_s$	27.3	24.1	–11.72	76.3	82.08
La4		$[\pm45/0_2]_{3s}$	29.5	28.98	–1.76	32.5	46.19
La5		$[(\pm45/0/90)_3]_s$	29.36	27.64	–5.86	21.2	36.700
La10		$[(0/90_2/0)_3]_s$	38.8	53	36.59	33.04	35.33

Fig. 8. Comparison among model methods with experimental data [25, 41] and other available models in compression based on Eq. (16).

TABLE 5. Comparison of Prediction of Fracture Toughness Based on Un-Notch Strength of Method 2

#	Material	Layup	Fracture toughness G_{IC}			ψ (GPa)	E_{eff} (GPa)
			Exp.	Predicted	% error		
La0	IM7/8552 [5, 33]	$[90/0/\pm45]_{3s}$	81.5	87.52 Eq. (17)	7.39	23.34	23.34
				Eq. (18)			
La3, doubled 0º	T800/924C [25, 41]	$[\pm45/0_2/90_2/0_2/90_2/0_2]_s$	27.3	25	−8.42	76.3	91.6
La4		$[\pm45/0_2]_{3s}$	29.5	23.7	−19.66	55.8	101
La5		$[(\pm45/0/90)_3]_s$	29.36	30.9	5.25	36.7	77.9
La10		$[(0/90_2/0)_3]_s$	38.8	36.09	−6.98	33.02	38.34

TABLE 6. Optimum Values for Fracture Toughness

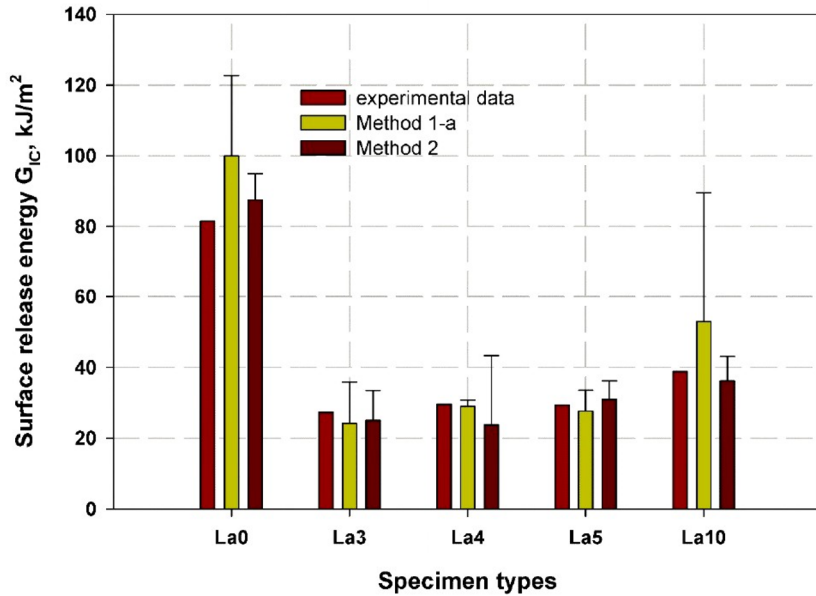| #	Material	Layup	Fracture toughness GIC			Method
			Exp.	Predicted	% error	
La0	IM7/8552 [5, 33]	$[90/0/\pm45]_{3s}$	81.5	87.52 Eq. (17)	7.39	2
				Eq. (18)		
La3, doubled 0º	T800/924C [25, 41]	$[\pm45/0_2/90_2/0_2/90_2/0_2]_s$	27.3	25.0	−8.42	2
La4		$[\pm45/0_2]_{3s}$	29.5	23.7	−1.76	1
La5		$[(\pm45/0/90)_3]_s$	29.36	30.9	5.25	2
La10		$[(0/90_2/0)_3]_s$	38.8	36.09	−6.98	2

Fig. 9. Comparison among model methods with experimental data [25, 26, 41] to predict the fracture toughness of different CFRP laminates.

The linear cohesion law provides considerable data for predicting the nominal strength of open-hole CFRP laminate structures. The cohesion law methods must define two main material properties, the notched impact strength and the fracture toughness G_{IC}, and the value of the nominal strength differs from the method in which the equivalent Young modulus is calculated, even in the present study [25, 41]. Figures 11 and 12 show the nominal strength of the open hole predicted using the calculated Young modulus ψ and the effective Young modulus E_{eff} based on

method 1-a and method 2, respectively. The percent error values for the open hole strength were 6.17 and –1.03 for La0. However, different percent error values were obtained for the other specimens, which can be attributed to the changed values of ψ and E_{eff}. The optimal values are listed in Table 7. It can be seen that the optimal values obtained by method 1-a with the equivalent Young modulus ψ for samples La3 and La10 have a percent error of 7.67 and –2.5, respectively. The percent error determined by method 2 with the equivalent Young modulus E_{eff} for La4 was 2.5, while it was 5.67 for La5 with the equivalent Young modulus ψ.
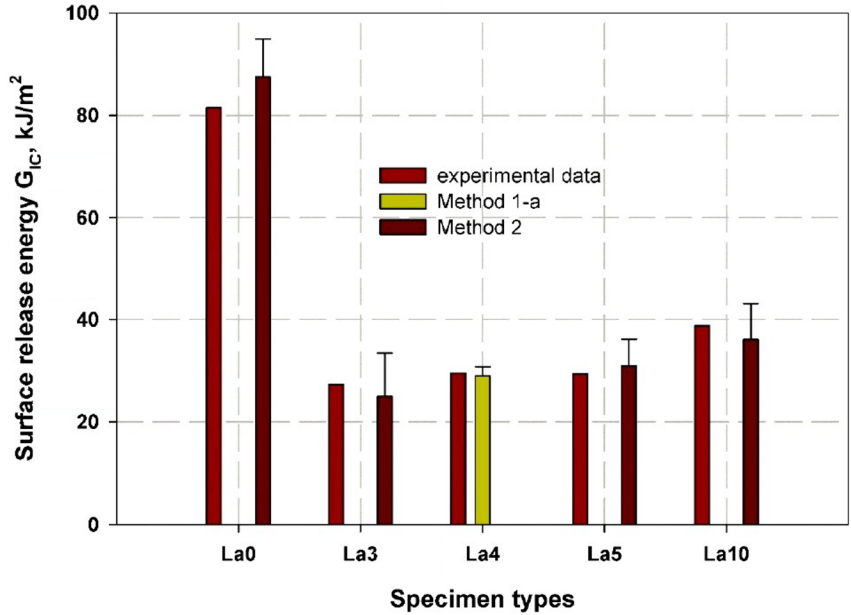

Fig. 10. Optimum values of the fracture toughness of different CFRP laminates with different methods and experimental data [25, 26, 41].
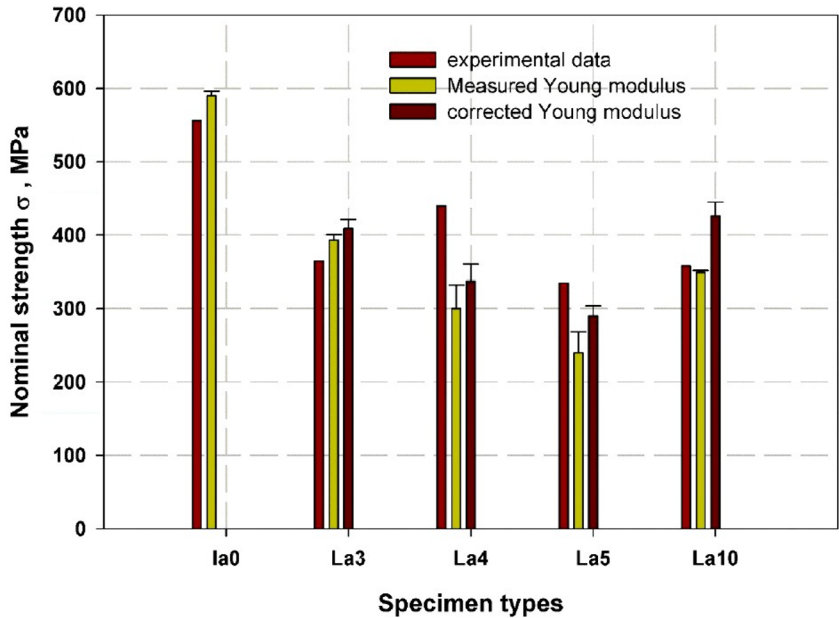

Fig. 11. Nominal strength of open hole CFRP laminates predicted based on un-notch strength calculated by method 1-a respect to experimental data [25, 26, 41].

1042

TABLE 7. Optimum Values for Open Hole Strength

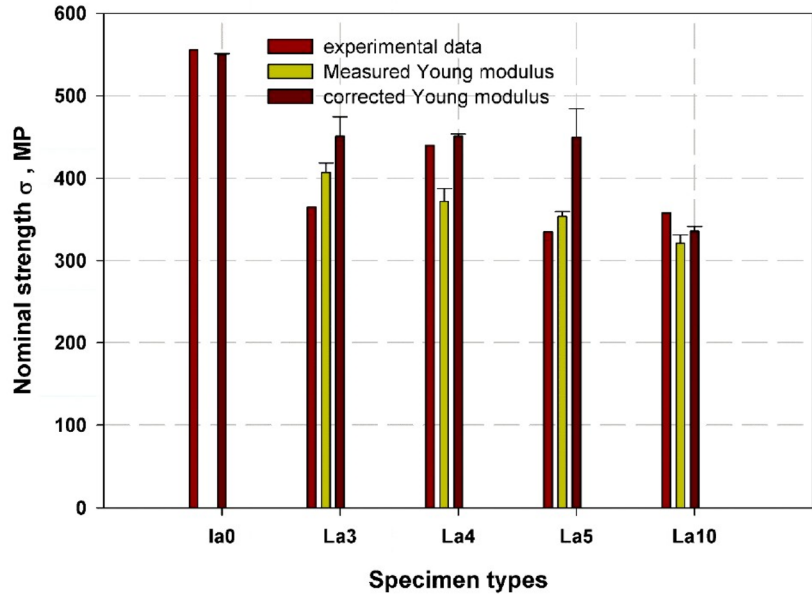| #	Material	Layup	Open hole strength			Method	Young modulus
			Exp.	Predicted	% Error		
La0	IM7/8552 [5, 33]	$[90/0/\pm45]_{3s}$	555.7	555.7	−1.02	2	ψ or E_{eff}
La3	T800/924C	$[\pm45/0_2/90_2/0_2/90_2/0_2]_s$	365	393	7.67	1	ψ
La4	[25, 41]	$[\pm45/0_2]_{3s}$	440	451	2.5	2	E_{eff}
La5		$[(\pm45/0/90)_3]_s$	335	354	5.67	2	ψ
La10		$[(0/90_2/0)_3]_s$	358	349	−2.51	1	ψ

Fig. 12. Nominal strength of open hole CFRP laminates predicted based on un-notch strength calculated by method 2 respect to experimental data [25, 26, 41].
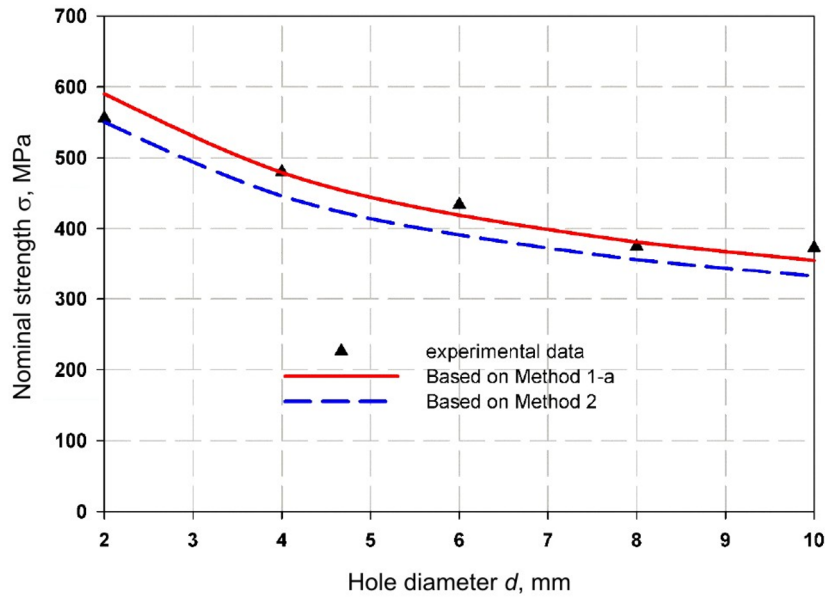

Fig. 13. Size effect curve prediction using un-notch and fracture toughness calculated with the proposed model compared to experimental data [26].

Figure 13 shows the size effect curve predicted using the linear cohesion law based on the predicted notched impact strength by method 1-a and method 2. Although the two methods provide a remarkably good prediction, method 1-a fits better due to its good fracture toughness and low notched impact strength predicted with a lower % error of 822. The average % accuracy of size effect prediction based on method 1-a is 3.24%, while it is 6.82% for method 2.

Conclusions. The notched impact strength of CFRP is a very important characteristic property, so it is of great importance to determine it. In the present study, it was predicted using two simple analytical methods based on the elastic strength and stiffness of unidirectional plies with an angle of 0° and lamination theory. A comparison study was proposed to determine the degree of accuracy of each method. Based on the predicted strength of different CFRP material systems and different layers, both the fracture toughness curve (G_{IC}) and the size effect curve were defined and the following optimal results were reported:

1. The second method, based on the ply ratio and force analysis through the whole laminate plate, is more suitable and gives a lower % error.

2. The maximum failure shear stress theory is well suited for CFRP laminates with higher fracture toughness, while the maximum principal failure stress theory is better suited for materials with fracture toughness of 25–40 kJ/m².

3. The equivalent modulus of elasticity, calculated based on the percentage of plies in the elastic stiffness of the laminates using the laminate theory, is well suited to measure open hole strength.

4. The average percentage accuracy of predicting the size effect based on method 1-a is 3.24%, while it is 6.82% for method 2.

REFERENCES

1. Y. Mohammed, M. K. Hassan, H. A. El-Ainin, and A. M. Hashem, "Size effect analysis of open-hole glass fiber composite laminate using two-parameter cohesive laws," *Acta Mech*, **226**, No. (4), 1027–1044 (2015).
2. R. Bhattacharyya and D. Adams, "Multiscale analysis of multi-directional composite laminates to predict stiffness and strength in the presence of micro-defects," *JCOMC*, **6**, 100189 (2021).
3. T. Q. Bui and X. Hu, "A review of phase-field models, fundamentals and their applications to composite laminates," *Eng Fract Mech*, **248**, 107705 (2021).
4. T. Bian, Q. Lyu, X. Fan, et al., "Effects of fiber architectures on the impact resistance of composite laminates under low-velocity impact," *Appl Compos Mater*, **29**, 1125–1145 (2022).
5. C. Furtado, A. Arteiro, M. A. Bessa, et al., "Prediction of size effects in open-hole laminates using only the Young's modulus, the strength, and the *R*-curve of the 0 ply," *Compos Part A-Appl Sci*, **101**, 306–317 (2017).
6. M. Y. Abdellah, "Delamination modeling of double cantilever beam of unidirectional composite laminates," *J Fail Anal Preven*, **17**, No. 5, 1011–1018 (2017).
7. A. Cutolo, A. R. Carotenuto, S. Palumbo, et al., "Stacking sequences in composite laminates through design optimization," *Meccanica*, **56**, No. (6), 1555–1574 (2021).
8. F.-L. Guo, P. Huang, Y.-Q. Li, et al., "Multiscale modeling of mechanical behaviors of carbon fiber reinforced epoxy composites subjected to hygrothermal aging," *Compos Struct*, **256**, 113098 (2021).
9. C. Soutis, N. Fleck, and P. Smith, "Failure prediction technique for compression loaded carbon fibre-epoxy laminate with open holes," *J Compos Mater*, **25**, No. 11, 1476–1498 (1991).
10. M. K. Hassan, Y. Mohammed, T. M. Salem, and A. M. Hashem, "Prediction of nominal strength of composite structure open hole specimen through cohesive laws," *Int J Mech Mech Eng IJMME-IJENS*, **12**, 1–9 (2012).
11. P. Rozylo, "Experimental-numerical study into the stability and failure of compressed thin-walled composite profiles using progressive failure analysis and cohesive zone model," *Compos Struct*, **257**, 113303 (2021).
12. S. Tan, "Effective stress fracture models for unnotched and notched multidirectional laminates," *J Compos Mater*, **22**, No. 4, 322–340 (1988).
13. Z. P. Bažant and Q. Yu, "Designing against size effect on shear strength of reinforced concrete beams without stirrups: I. Formulation," *J Struct Eng*, **131**, No. 12, 1877–1885 (2005).

14. J. Planas and M. Elices, "Asymptotic analysis of a cohesive crack: 2. Influence of the softening curve," *Int J Fract*, **64**, No. 3, 221–237 (1993).

15. Y. Mohammed, M. K. Hassan, H. A. El-Ainin, and A. M. Hashem, "Size effect analysis in laminated composite structure using general bilinear fit," *Int J Nonlinear Sci Numer Simul*, **14**, Nos. 3–4, 217–224 (2013).

16. D. Fanteria, L. Lazzeri, E. Panettieri, et al., "Experimental characterization of the interlaminar fracture toughness of a woven and a unidirectional carbon/epoxy composite," *Compos Sci Technol*, **142**, 20–29 (2017).

17. E. Özaslan, M. A. Güler, A. Yetgin, and B. Acar, "Stress analysis and strength prediction of composite laminates with two interacting holes," *Compos Struct*, **221**, 110869 (2019).

18. P. P. Camanho, G. H. Erçin, G. Catalanotti, et al., "A finite fracture mechanics model for the prediction of the open-hole strength of composite laminates," *Compos Part A-Appl Sci*, **43**, No. 8, 1219–1225 (2012).

19. G. H. Erçin, P. P. Camanho, J. Xavier, et al., "Size effects on the tensile and compressive failure of notched composite laminates," *Compos Struct*, **96**, 736–744 (2013).

20. Z. P. Bažant, "Size effect," *Int J Solid Struct*, **37**, Nos. 1–2, 69–80 (2000).

21. Z. P. Bazant and E.-P. Chen, "Scaling of structural failure," *Appl Mech Rev*, **50**, No. 10, 593–627 (1997).

22. P. Camanho and G. Catalanotti, "On the relation between the mode I fracture toughness of a composite laminate and that of a 0 ply: analytical model and experimental validation," *Eng Fract Mech*, **78**, No. 13, 2535–2546 (2011).

23. Y. Mohammed, M. K. Hassan, and A. Hashem, "Analytical model to predict multiaxial laminate fracture toughness from 0 ply fracture toughness," *Polym Eng Sci, 54*, No. 1, 234–238 (2014).

24. M. Y. Abdellah, "Comparative study on prediction of fracture toughness of CFRP laminates from size effect law of open hole specimen using cohesive zone model," *Eng Fract Mech*, **191**, 277–285 (2018).

25. C. Soutis and P. Curtis, "A method for predicting the fracture toughness of CFRP laminates failing by fibre microbuckling," *Compos Part A-Appl Sci*, **31**(, No. 7, 733–740 (2000).

26. P. P. Camanho, P. Maimí, and C. Dávila, "Prediction of size effects in notched laminates using continuum damage mechanics," *Compos Sci Technol*, **67**, No. 13, 2715–2727 (2007).

27. S. Jose, R. Ramesh Kumar, M.K. Jana, and G. Venkateswara Rao, "Intralaminar fracture toughness of a cross-ply laminate and its constituent sub-laminates," *Compos Sci Technol*, **61**, No. 8, 1115–1122 (2001).

28. K. D. Cowley and P. W. Beaumont, "The interlaminar and intralaminar fracture toughness of carbon-fibre/polymer composites: the effect of temperature," *Compos Sci Technol*, **57**, No. 11, 1433–1444 (1997).

29. A. C. Garg, "Intralaminar and interlaminar fracture in graphite/epoxy laminates," *Eng Fract Mech*, **23**, No. 4, 719–733 (1986).

30. M. Y. Abdellah, "An approximate analytical model for modification of size effect law for open-hole composite structure under biaxial load," *P I Mech Eng C-J Mec*, **235**, No. 18, 3570–3583 (2021).

31. P. R. Barnett, S. A. Young, N. J. Patel, and D. Penumadu, "Prediction of strength and modulus of discontinuous carbon fiber composites considering stochastic microstructure," *Compos Sci Technol*, **211**, 108857 (2021).

32. M. Y. Abdellah, M. K. Hassan, A. F. Mohamed, and K. A. Khalil, "A novel and highly effective natural vibration modal analysis to predict nominal strength of open hole glass fiber reinforced polymer composites structure," *Polymers*, **13**, No. 8, 1251 (2021).

33. P. P. Camanho and M. Lambert, "A design methodology for mechanically fastened joints in laminated composite materials," *Compos Sci Technol*, **66**, No. 15, 3004–3020 (2006).

34. C. G. Dávila, C. A. Rose, and P. P. Camanho, "A procedure for superposing linear cohesive laws to represent multiple damage mechanisms in the fracture of composites," *Int J Fracture*, **158**, No. 2, 211–223 (2009).

35. Z. P. Bažant, "Size effect in blunt fracture: concrete, rock, metal," *J Eng Mech*, **110**, No. 4, 518–535 (1984).

36. G. T. Hahn and A. R. Rosenfield, "Local yielding and extension of a crack under plane stress," *Acta Metall Mater*, **13**, No. 3, 293–306 (1965).

37. N. Perez, *Crack Tip Plasticity*, in: *Fracture Mechanics*, Springer (2017), pp. 187–225.

38. B. Esp, *Stress Distribution and Strength Prediction of Composite Laminates with Multiple Holes*, The University of Texas at Arlington (2007).

39. V. Birman and G. M. Genin, *1.15 Linear and Nonlinear Elastic Behavior of Multidirectional Laminates*, in: P. W. R. Beaumont and C. H. Zweben (Eds.), *Comprehensive Composite Materials II*, Vol. 1, Academic Press, Oxford (2018), pp. 376–398.

40. R. Amacher, J. Cugnoni, J. Botsis, et al., "Thin ply composites: experimental characterization and modeling of size-effects," *Compos Sci Technol*, **101**, 121–132 (2014).

41. P. Berbinau and C. Soutis, "A study of 0°-fibre microbuckling in multidirectional composite laminates," in: Proc. of the Twelfth Int. Conf. on Composite Materials (ICCM-12, Paris, France, July 5–9, 1999), Paper 237 (1999).

42. S. Biswas and A. Satapathy, "A comparative study on erosion characteristics of red mud filled bamboo–epoxy and glass–epoxy composites," *Mater. Design*, **31**, No. 4, 1752–1767 (2010).

43. A. L. Fairchild, D. Rosner, J. Colgrove, et al., "The EXODUS of public health what history can tell us about the future," *Am J Public Health*, **100**, No. 1, 54–63 (2010).

44. C. Furtado, A. Arteiro, G. Catalanotti, et al., "Selective ply-level hybridisation for improved notched response of composite laminates," *Compos Struct*, **145**, 1–14 (2016).